PERGAMON International Journal of Multiphase Flow 25 (1999) 1521–1543

International Journal of Multiphase Flow

www.elsevier.com/locate/ijmulflow

Analysis of dryout in horizontal and inclined tubes

A. Mosyak*, G. Hetsroni

Faculty of Mechanical Engineering, Technion, Israel Institute of Technology, Haifa 32000, Israel

Received 12 May 1998; received in revised form 30 November 1998

Abstract

The infrared thermography technique was used to study the thermal and hydrodynamic phenomena in intermittent two-phase air–water flow in horizontal and inclined tubes at atmospheric pressure. The study was aimed at elucidating the relationship between the hydrodynamic parameters and dryout phenomena. It focuses on the empirical evaluation of the wall temperature distribution in a uniformly heated pipe. The results reveal the existence of dryout phenomena in horizontal pipe flow only. The flow parameter based on the frequency, length and velocity of elongated bubble is presented for the prediction of dryout.

1. Introduction

Refilling and rewetting is of fundamental importance for the re-establishment of normal and safe temperature levels following dryout in heated pipelines carrying gas and liquid simultaneously. Intermittent flows of gases and liquids occur in steam (condensing) flows, particularly, in horizontal or moderately upward tilted absorber tubes of solar power plants (Hahne et al., 1997). Parabolic trough solar power plants using thermal oil as primary heat transfer medium have attained a state-of-the-art, where further technical development would yield only slight cost reductions. Direct steam generation (DSG) process has a large potential to increase efficiency and to reduce cost by generating live steam for the turbine, in the absorber tubes of the parabolic collectors. This two-phase flow exhibits a typical thermohydraulic behavior, i.e. an intermittent flow may occur. Liquid holdup, pressure gradient, angles of inclination and the film dryout are the key parameters in the design, scale-

* Corresponding author.

0301-9322/99/$ - see front matter
PII: S0301-9322(98)00081-0

up and control of the two-phase flow in horizontal and inclined tubes, and in the prevention of potentially detrimental phenomena such as dryout.

An important and well-recognized concept in dealing with intermittent gas–liquid pipe flows is that of flow patterns (Barnea and Taitel, 1986). The interfacial instabilities for horizontal gas–liquid flows in pipelines were studied by Andritsos and Hanratty (1987), the effect of surface tension on flow pattern, hold-up and pressure drop during horizontal air–water pipe flow was investigated by Hand et al. (1992), and Hand and Spedding (1993). Experimental results of the investigations of the effect of liquid viscosity on the phase distribution in two-phase air–liquid slug flow in horizontal pipes are presented by Nadler and Mewes (1995). An experimental study of two-phase flow in slightly inclined tubes was carried out by Kokal and Stanislav (1989). Taitel and Barnea (1990) published the model, which permits the prediction of pressure drop in inclined slug flow. Andreussi et al. (1993) presented a mechanistic model of slug inclined flow in near-horizontal pipelines. The modified apparent rough surface model was presented by Grolman and Fortuin (1997a, 1997b), which facilitates prediction of liquid hold-up and pressure gradient in gas–liquid flow through horizontal and slightly sloping pipes.

The study of dryout heat transfer has received considerable attention because of its importance in determination of maximum wall temperature in chemical process equipment, conventional and nuclear power generation systems, refrigeration plants and other industrial devices. Slug flow boiling is usually encountered at low flows and void fractions which are too high to maintain inverted annular film boiling, but too low to maintain dispersed flow film boiling. In tubes it is formed just downstream of the inverted annular flow regime when the liquid breaks up into slugs of liquid between bubbles of vapor. Knowledge of the wall-boundary condition and phase distribution is important in predicting two-phase heat transfer and pressure drop, it is also necessary to know the conditions under which the wall undergoes a dryout. Slug flow or intermittent dryout is accompanied by oscillations in pipe temperature which may be, in fact, more damaging than high absolute temperatures. Fisher and Yu (1975) studied intermittent dryout using higher pressure R-12. Ruder et al. (1986) and Bar-Cohen et al. (1987) found intermittent dryout boundaries for atmospheric steam–water in a 25.4 mm horizontal tube. Crowe and Griffith (1993) determined the dryout limits in horizontal tube with emphasis on the effects of pipe size and flux.

The initial attempts on physically based dryout models have been made by Coney (1974) and Ruder et al. (1986). Coney (1974) presented a fluid mechanical analysis where emphasis is given on the initial after-slug film thickness and the inertial effects in the falling film. Ruder et al. (1986) considered two effects tending to remove liquid from the wall, namely the post-slug liquid film drainage down the tube wall and evaporation of this film driven by the imposed heat flux. Surprisingly, little work has been done which relates the film dryout to the slug unit properties, e.g. elongated gas bubble, liquid slug, bubble velocity and frequency. The study of Crowe and Griffith (1993) included effect of slug frequency on dryout, but effect of bubble size and velocity was not investigated.

Recent data give indication that in the dryout region of boiling, there may be, in fact, heat transfer from the wall to the gas phase only. Here, we present information on dryout in intermittent air–water flow. The real system, which is associated with the evaporation of water flowing in pipes, is different in the sense that the quality is changing along the pipes due to the heating. An experiment of actual heating of steam–water mixture is very costly and we learn

about the basic behavior from a water–air system where the air simulates the vapor. The prediction of the dryout in such a case is important to study the hydrodynamic conditions of the breakup of inverted annular flow.

In order to advance the study of dryout and its effect on heat transfer, one needs to study the temperature patterns on the heated tube as a function of the flow rate, heat flux, etc. The analysis must connect the hydrodynamic phenomena with dryout conditions that occur for intermittent flow in horizontal and inclined tubes. This has motivated the present study which provides a better understanding of the physical phenomena that occur in an intermittent dryout system. The experiments and the model were used to consider a relatively simple problem with well known hydrodynamic parameters of two-phase air–water flow. From photographic studies, which will be discussed later, the bubble size, bubble frequency and bubble velocity can be identified and the local heat transfer processes can be connected with flow pattern. In this case, we do not have to consider the mass transfer terms.

2. Heat transfer and dryout problem

2.1. The quasi-steady-state analysis approach to the dryout problem

The studies of steady-state convective heat transfer focused on the effect of numerous factors, including many geometries, internal and external boiling, forced and free convection, mixtures of fluids, and various hydraulic conditions (Hewitt and Wallis, 1974; Elias and Yadigaroglu, 1977; Chan and Banerjee, 1981; Hetsroni, 1982). A comprehensive review and discussion to its relationship to boiling is given by Nelson and Pasamehmetoglu (1992). The important reason for the quasi-steady-state approach arises from the difficulty in obtaining a solution to the transient convection problem for two-phase situations.

We will discuss the question in terms of the interface between the two-phase fluid (liquid–gas) and the wall. For this, consider the transient local heat flux as

$$q = q(\tau, T_w, T_f, p, G, \varepsilon_v \dots) \tag{1}$$

where q is the total heat flux from the wall, τ is the time, T_w is the wall temperature, T_f is the fluid temperature, p is the pressure, G is the total mass flux, and ε_v is the vapor volumetric void fraction.

When $G = \varepsilon = 0$, p and T_f are constant, the total derivative of (1) with respect to time can be written as

$$\frac{dq}{d\tau} = \left(\frac{\partial q}{\partial T_w}\right)\left(\frac{dT_w}{d\tau}\right) \tag{2}$$

This equation has been discussed by Nelson and Pasamehmetoglu (1992) relative to the application of the quasi-steady-state model for the convection problem.

In general, the term dryout indicates a local continuous contact of the gas phase with the surface. This term contains no statement as to the average (either spatial or temporal) value of

the surface temperature at which dryout may occur. The term used in the present study is defined with respect to averaged viewpoint of the process time.

It is worthwhile to develop some understanding of certain aspects of the more general topic of two-phase modeling and the assumptions which are involved. For a review of this general topic, the work of Ishii (1975) and Delhaye (1981) provides excellent summaries. Our discussion will be limited to the definition of heat transfer coefficient, because it is the averaging value for which the dryout must be specified. Since the microscopic details of this process are rarely needed for engineering problems, the macroscopic nature of the process is usually much more important. The averaging operation effectively eliminates information on local instantaneous fluctuation. Eulerian averaging is of the group that is of most interest to us in this study, because it involves averaging over time and space, which are the independent variables. In the present study, we use time-averaged value of the heat transfer coefficient at a fixed point located at the angle $\theta = 2\varphi/\pi$, where φ is the angle from the top of the pipe:

$$\alpha_\theta = \frac{1}{\tau}\int_0^\tau \alpha(\tau)\,\mathrm{d}\tau \tag{3}$$

and time and space mean value, of heat transfer coefficient within the angle θ and $\theta + \Delta\theta$:

$$\alpha_{\Delta\theta} = \frac{1}{\tau\Delta\theta}\int_0^\tau\int_\theta^{\theta+\Delta\theta} \alpha(\tau,\theta)\,\mathrm{d}\tau\,\mathrm{d}\theta \tag{4}$$

If dryout is present in intermittent flow, the averaged heat transfer coefficient at the top of the tube has contributions from convection of both liquid and gas phases. Since the heat transfer coefficient to water is substantially higher than that to a gas, the average heat transfer coefficient under dryout conditions is lower, leading to a higher time-average wall temperature under uniform heat flux conditions. In this case the space-averaged heat transfer coefficient for air–water flow on the upper part of the tube $\alpha_{\Delta\theta}$ may be written in the following way:

$$\alpha_{\Delta\theta} = \frac{1}{F}\left[\alpha_\mathrm{d}F_\mathrm{d} + \alpha_0(F - F_\mathrm{d})\right] \tag{5}$$

Taking into account that $\alpha_\mathrm{d} \ll \alpha_0$ we obtain

$$\frac{\alpha_{\Delta\theta}}{\alpha_0} = \frac{(F - F_\mathrm{d})}{F} \tag{6}$$

For determination of dryout we used the relation of the time-averaged heat transfer coefficients on the top and bottom as a criterion. It was assumed that relation $\alpha_{\Delta\theta}/\alpha_0 < 1$ indicates dryout, i.e. the surface superheat $\bar{T}_\mathrm{w} - \bar{T}_\mathrm{f}$ is greater than that, when the surface contacts single-phase water only. This method can be applied to connect dryout with hydraulic conditions, if the value of $\alpha_{\Delta\theta}$ may be associated with intermittent flow parameters.

2.2. Relationship between heat transfer on the upper part of the tube and hydrodynamics

A two-phase intermittent flow is commonly defined as a flow in which gas phase is distributed within a liquid continuum. A schematic geometry of slug flow is shown in Fig. 1.

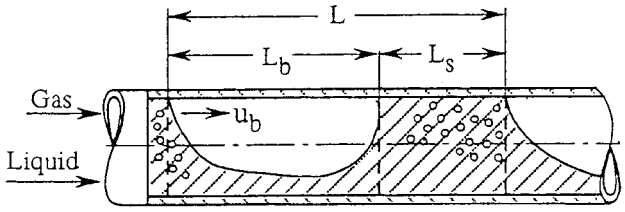

Fig. 1. Simplified slug model.

The slug body, L, is subdivided into two main sections: the liquid slug zone of length L_s and the bubble zone of length L_b. The liquid holdup within the bubble zone is designated as $\varepsilon = 4A/\pi d^2$, where A is cross-sectional area of the liquid phase. In order to predict the heat transfer in horizontal and inclined pipes, it is important to elucidate the turbulent structure of the continuous liquid phase. Although the liquid slug zone can be aerated by dispersed bubbles, it forms a competent bridge and gas cannot penetrate through the slug zone. The purpose of modeling heat transfer must be fairly close to the true physical process that is taking place, but it is also important for a model to be simple enough so that analytical parameters could be compared with experimental data.

As a first step toward the understanding of the local heat transfer mechanisms, we propose to subdivide the heat transfer phenomenon in the intermittent flow into two components: one due to the residence of liquid slug, and the other due to effects caused by the bubble motion. For horizontal and inclined pipes an elongated gas bubble is in the upper part of the pipe. Intermittent flow consists of liquid slugs and gas bubbles which are usually greater in length than one pipe diameter. The liquid may or may not contain dispersed bubbles, depending on the gas and liquid flow rates. Our analysis concerns the elongated bubble regime. In the case of air–water intermittent flow, the time-average two-phase heat transfer coefficient at the fixed point α_θ on the upper part of the tube will depend on the mean air-phase heat transfer coefficient α_b, liquid slug mean heat transfer coefficient α_s, and the time periods $\Delta\tau_b$,$\Delta\tau_s$ that takes for air and liquid slug to pass a fixed point. The time-average air–water two-phase heat transfer coefficient on the upper part of the tube may be written in the following way:

$$\alpha_\theta = \frac{1}{\tau}(\alpha_b \Delta\tau_b + \alpha_s \Delta\tau_s) \tag{7}$$

where $\tau = \Delta\tau_s + \Delta\tau_b$ represents time-averaging interval. When the time-averaging interval is short, it is possible to distinguish wetting or drying of the surface. When the time-averaging interval is long enough, dryout affects overall heat transport phenomena. Because hydraulic phenomena in intermittent flow has periods associated with slug unit frequency, f_s, the time-averaging interval must be $\tau \gg 1/f_s$.

If L_i is the length of the slug, then $\Delta\tau_b$ is given by

$$\Delta\tau_b = \frac{1}{u_b}\sum_{i=1}^{N} L_i \tag{8}$$

where N is the number of bubbles passing a fixed point during time period τ, u_b is the bubble velocity, and L_i is the bubble length. Eq. (8) assumes that u_b is independent of L_i. The validity of this assumption has been shown in the previous studies by Hetsroni et al. (1998a, 1998b).

Define the bubble-average length L and the frequency of bubble appearance f as

$$L = \frac{1}{N}\sum_{i=1}^{N} L_i \tag{9}$$

$$f = \frac{1}{\tau}N \tag{10}$$

From Eqs. (8)–(10) one can obtain:

$$\frac{\Delta\tau_b}{\tau} = \frac{fL}{u_b} \tag{11}$$

Using Eq. (11), the Eq. (7) can be expressed as

$$\frac{\alpha_\theta}{\alpha} = \frac{\alpha_s}{\alpha}\left(1 - \frac{fL}{u_b}\right) + \frac{\alpha_b}{\alpha}\frac{fL}{u_b} \tag{12}$$

where α is the heat transfer coefficient for the single-phase liquid, $R = fL/u_b$ is the ratio of the time for gas phase (elongated air bubbles) to pass the fixed point to the total time for air and water mixture, and $(1 - fL/u_b)$ is the ratio of the time for water slugs to pass the fixed point to the total time.

It should be noted that the liquid-slug heat transfer coefficient α_s may be different from α. The water slugs may contain many dispersed bubbles, which will increase the water-phase turbulence level and convection heat transfer coefficient. When the elongated bubble passes the fixed-point convection heat, transfer will be highly dependent on the physical properties of the flow, that is viscosity, density, surface tension of the fluid, and the ratio of fL/u_b. Depending on these parameters the wetting of the upper surface may occur even while an elongated bubble is in the place. In this case, the average surface superheat $\bar{T}_w - \bar{T}_f$ may be less than that for clear water. The scope of the present analysis is limited to the prediction of dryout in air–water flow.

Therefore, these results are not sufficient to generalize the effects of the liquid viscosity and surface tension on the slug characteristics and dryout. We believe that the ratio of time for air to pass the fixed point to the total time of slug unit is the main parameter to determine whether or not dryout takes place. Thus, the equation

$$\frac{\alpha_\theta}{\alpha} < 1 \tag{13}$$

indicates a dryout process.

3. Experimental arrangement

3.1. Flow facility

A flow facility was specially constructed to study the effect of dryout in horizontal and inclined tube up to $\beta = 5^\circ$. In this facility, shown schematically in Fig. 2, the two-phase flows of water and air were investigated by changing flow rates of the phases. The volumetric flow rates of both phases could be regulated independently and were measured by flow meters. Filtered air was drawn from a constant pressure receiver supplied from the compressed air main and introduced into the mixing section. Water was pumped from a supply tank and also introduced into the mixing section. The air–water mixture passed through the 3600-mm long development section of 49.2 mm internal diameter into 1200-mm long transparent glass section for flow visualization by a video technique. The heated section for temperature measurements was positioned behind the glass section. This section of 180 mm length was constructed from a 50-μm thick constantan foil and heated by direct-current. Special attention has been paid to the design of the heated section: the heat is not transported along the wall and the temperature of air–water mixture does not change significantly along the test section. That means, the test section must be made of thin wall and it should be short. Experiments in the horizontal tube were performed at the range of heat flux q from 0.7 to 19 kW/m^2, experiments in the inclined tube were performed in the range of heat flux q from 27 to 53 kW/m^2. There was no vaporization of the water film during the gas slug passage. The air and water emerging from the test section were separated in the tank, the air was released to atmosphere.

3.2. Measurement techniques

The motion of bubbles in the pipe was studied by analyzing video images. The method is based on the detection of the edges of the bubbles in a sequence of video frames. This method

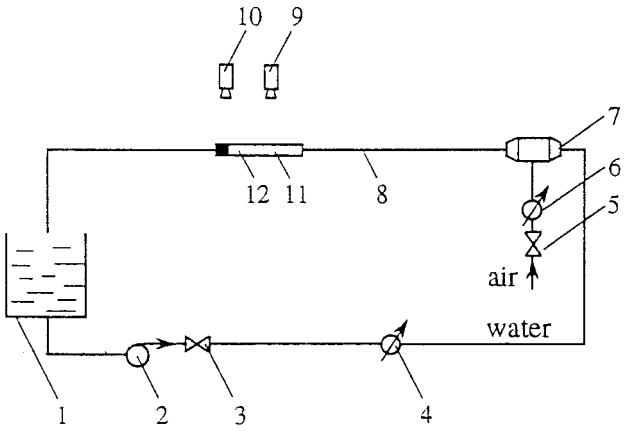

Fig. 2. Experimental facility: 1—tank, 2—pump, 3—flow regulator, 4—water flowmeter, 5—air regulator, 6—air flowmeter, 7—mixing section, 8—developemnt section, 9—video camera, 10—infra-red camera, 11—glass section, 12—heated test section.

allows to measure the length, size and velocity of elongated bubbles. The bubble motion of intermittent flow was recorded consecutively by a 3-CCD video camera. The illumination was provided by a set of 500-W halogen lamps, mounted on a frame at the opposite side of the test section. Pictures were taken with a black background, so that the bubbles had a white outline. The camera provided the video signal which consists of two fields, represented by the odd and even rows of the image, respectively. Each video frame thus produces two bubble images at the effective sampling frequency of 50 Hz. In each run a sequence of at least 120 s was recorded. In the playback mode, typical flow patterns were frozen on the TV monitor and analyzed frame by frame to calculate the average length, height and frequency for each set of the data.

At low gas velocities, the flow consisted of elongated gas bubbles which move along the upper part of the pipe. Neglecting aeration, in developing necessary conditions for the existence of slugging, may introduce errors in the analysis of the slugging front and tail behavior. However, for the case of moderate aeration, this simplification may not be too serious (Ruder et al., 1989).

A Thermal Imaging Radiometer was used in the investigation of the thermal patterns. It has a typical horizontal and vertical resolution of 256 pixels per line. The radiometer allows one to obtain a qualitative thermal profile in the line mode, the average temperature in the area mode, and the temperature of a given point in the point mode. No calibration correction for a curved surface is required.

The experiments were carried out at a constant heat flux. We had to consider the frequency response of the system to changes in the heat transfer coefficient. For this purpose, we solved numerically the transient heat conduction problem. The magnitude of the heat transfer coefficient is proportional to $cs(f\tau)$ where f is the frequency and τ is the time. It was shown by Hetsroni and Rozenblit (1994) and Hetsroni et al. (1996) that temperature distortions and phase shift in temperature fluctuations on the heated wall begin at $f = 15$–$20\ \mathrm{s}^{-1}$. In the present study the highest frequency of bubbles did not exceed $7\ \mathrm{s}^{-1}$.

The surface temperature and the air–water mixture temperature were measured with an accuracy of $\pm 0.1^{\circ}\mathrm{C}$. The water flow was controlled by a valve and measured by a standard orifice plate with an accuracy of $\pm 1\%$. The air flow was measured by means of a mass flowmeter with an accuracy of $\pm 1\%$. The pressure was measured by the pressure transducers with an accuracy of $\pm 1\%$. Electrical power was determined by means of a digital watt meter with an accuracy of $\pm 0.5\%$.

3.3. Data reduction and test procedure

A number of verification runs were undertaken prior to the data logging. A series of single-phase water flow test were made to establish the validity of the system and testing technique. The time-averaged heat transfer coefficient is defined as

$$\alpha = \frac{q}{\bar{T}_{\mathrm{w}} - \bar{T}_{\mathrm{f}}} \tag{14}$$

where q is the heat flux, $\bar{T}_{\mathrm{w}}$ is the time-averaged wall temperature, $\bar{T}_{\mathrm{f}}$ is the time-averaged mean value of the water temperature at the entrance and the exit of the section.

Two-phase tests were conducted for air–water flow in horizontal and inclined tube at $\beta = 5^\circ$, with various liquid and air flowrates. The distribution of bubble size becomes independent 83 diameters downstream of the mixing chamber.

The time-averaged local heat transfer coefficient in air–water flow is defined as

$$\alpha_\theta = \frac{q}{\bar{T}_\theta - \bar{T}_f} \tag{15}$$

where $\bar{T}_\theta$ is the time-averaged wall temperature at the angle θ. We carried out measurements of the heat transfer coefficient at different locations along the heated section. It was found that the ratio of the time-averaged heat transfer coefficient at the given point in air–water flow to the time-averaged heat transfer coefficient in clear water did not depend on the distance from the entrance of the heated section to the points of measurements. It should be noted that this technique has been the subject of a number of previous tests (Hetsroni et al., 1998a, 1998b) and found to be accurate. The average wall-shear stress τ_0 was calculated from the pressure drop measurements and the wall-shear velocity $u^* = (\tau_0/\rho)^{0.5}$ was computed.

4. Experimental results

4.1. Flow parameters

The experiments were performed in horizontal and upward inclined tube at $\beta = 5^\circ$. For horizontal flow, the superficial velocities of the liquid phase were $U_{LS} = 0.62$ to 1.40 m/s ($Fr_L = 0.9$–2.0), the superficial velocities of the air phase were $U_{GS} = 0.02$–0.30 m/s ($Fr_G = 0.03$–0.43). For flow into the inclined tube, the parameters were $U_{LS} = 0.40$–1.40 m/s ($Fr_L = 0.59$–2.0), $U_{GS} = 0.02$–0.39 m/s ($Fr_G = 0.03$–0.57). The Froude numbers are defined as $Fr_L = U_{LS}/\sqrt{gD}$, $Fr_G = U_{GS}/\sqrt{gD}$, D is the inner pipe diameter, g is acceleration due to gravity. According to the flow regime map, suggested by Barnea and Taitel (1986), the experiments for the air–water mixture in a horizontal pipe were carried out at the intermittent flow regime. The data for an inclination $+5^\circ$ correspond to intermittent regime with elongated bubbles (Taitel and Dukler, 1976). Flow parameters, such as length of the elongated bubbles, liquid hold-up within the bubbles, frequency of bubble appearance and bubble velocity, were determined by analyses of video pictures. For each flow condition, at least 300 individual data sets were recorded and the average values were calculated. These calculations were performed for the fully developed state, when the bubble size distribution did not change in the flow direction. For air–water flow in horizontal tube, the average values of bubble length within standard deviation of 15% agree with data of Barnea and Taitel (1993). The experimentally determined values of bubble velocity agree within a standard deviation of 11%, with correlation of Taitel and Barnea (1990). For air–water flow in inclined tube the bubble velocity is in good agreement (standard deviation of 10%) with results of Singh and Griffith (1970).

Figs. 3 and 4 show liquid holdup, ε_h and ε_{in}, as a function of the gas Froude number for various values of the liquid Froude number for horizontal and inclined tubes, respectively. The holdup was calculated based both on top and side views of large-length bubbles that touch the upper part of the wall and are separated by water slugs. The average data are presented. No

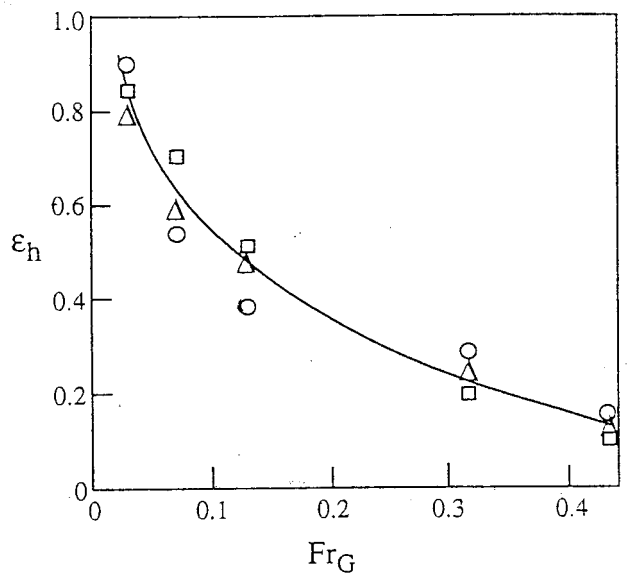

Fig. 3. Liquid holdup ε_h in horizontal tube as a function of gas Froude number: ○ $Fr_L = 0.9$, □ $Fr_L = 1.3$, △ $Fr_L = 2.0$.

significant influence of liquid Froude number is observed. This confirms the results from the experiments of Nicholson et al. (1978) in this range of gas and liquid Froude numbers. The fact that liquid holdup is independent of the superficial liquid velocity, indicates that under these conditions the mechanism of wave formation is independent of the liquid Froude

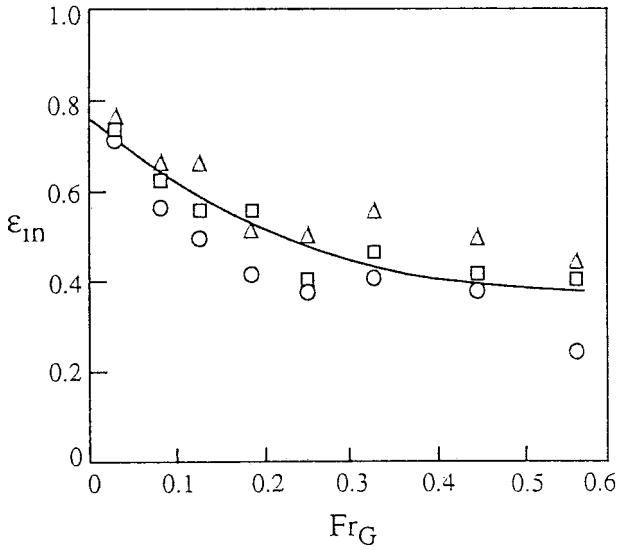

Fig. 4. Liquid holdup ε_{in} in inclined at $\beta = 5^\circ$ tube as a function of gas Froude number: ○ $Fr_L = 0.59$, □ $Fr_L = 1.2$, △ $Fr_L = 2.0$.

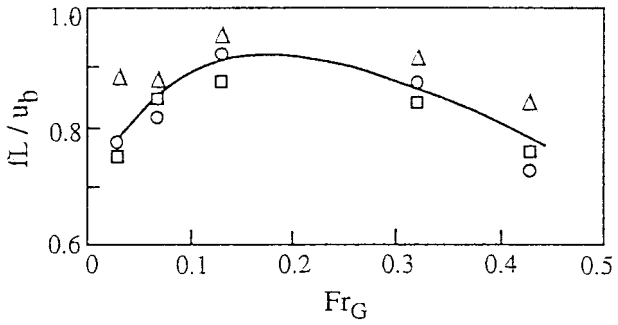

Fig. 5. Parameter fL/u_b vs. the gas Froude number in horizontal tube: ○ $Fr_L = 0.9$, □ $Fr_L = 1.3$, △ $Fr_L = 2.0$.

number. Experimental and analytical studies by Hanratty and Hershmann (1961), Dukler and Hubbard (1975) and Andreussi et al. (1985), have shown that, for a range of flow conditions over which an intermittent flow is observed, a wave is formed and grows rapidly to block the flow. These figures clearly demonstrate the effect that inclinations have, especially in the range of $Fr_G > 0.1$. For $Fr_G > 0.1$ the holdup in the inclined tube is much larger than that of the horizontal one. The holdup decreases as the superficial gas velocity increases. This phenomenon has also been observed by Lin and Hanratty (1987a, 1987b), and Jepson and Taylor (1993).

Figs. 5 and 6 show a plot of fL/u_b vs. the gas Froude number Fr_G at different liquid Froude numbers in horizontal and inclined tubes, respectively. It can be seen that the magnitude of fL/u_b for all regimes studied in a horizontal tube is much larger than that in an inclined tube. Since this parameter reflects the ratio of the time occupied by a bubble to the total residence time of a two-phase mixture at the top of the heated wall, the heat transfer in a horizontal tube, must be, generally, drastically reduced compared to that in an inclined tube.

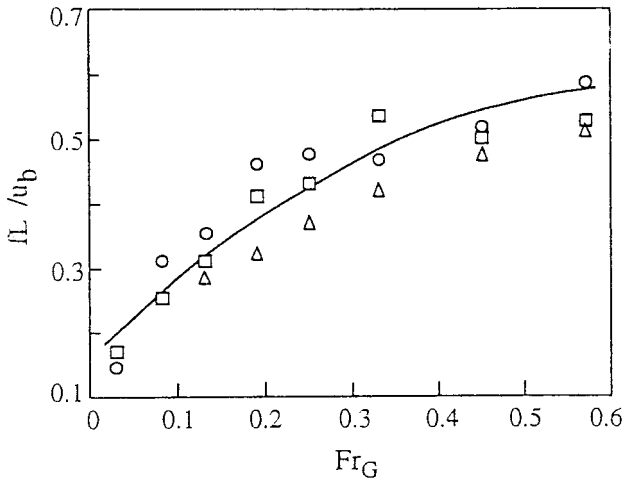

Fig. 6. Parameter fL/u_b vs. the gas Froude number in inclined tube: ○ $Fr_L = 0.59$, □ $Fr_L = 1.2$, △ $Fr_L = 2.0$.

4.2. Heat transfer and dryout

In Fig. 7 the ratio of the time-averaged heat transfer coefficient at the top of the tube to that for single-phase liquid, $\alpha_\theta = \alpha_0/\alpha$, is plotted against gas Froude number. The open symbols denote the data for horizontal tube, the closed symbols denote the data for inclined tube, the time-average interval is $\tau = 300$ s. On the top of the inclined tube the time-averaged heat transfer coefficient for air–water mixture is higher than that for clear water.

The heat transfer coefficient from the wall is governed by Eq. (12) and the results provide an adequate representation of dryout process described by Eq. (13). If definition of dryout as time-average problem is acceptable and Eq. (13) can be applied, one can see that in inclined tube no dryout problem occurs. Thus, in the present study the connection between heat transfer coefficient and dryout is restricted to air–water flow in horizontal tube. Fig. 8 shows the dependence of the ratio $((F - F_d)/F)$ of the wet surface $(F - F_d)$ to the total surface F, on the liquid flow Froude number Fr_L. Experimental points display results at the top of the horizontal tube within the angle $0 \leq \theta \leq 0.055$ in the range of gas Froude number $Fr_G = 0.03$–0.43. It can be seen that the part of wet surface increases with increasing liquid Froude number, Fr_L. For $Fr_L = 2$ the value of no dryout surface is about 90% of the whole heated surface. This result is in good agreement with the prediction of low-quality dryout in horizontal boiler tubes proposed by Ruder et al. (1986). They found experimentally that the upper limit of liquid Froude number, when the wall becomes circumferentially non-isothermal at $Fr_L > 2$.

Dryout of the liquid film on the upper surface changes in the circumferential direction. This hydrodynamic phenomenon leads to circumferentially non-uniform distribution of heat transfer

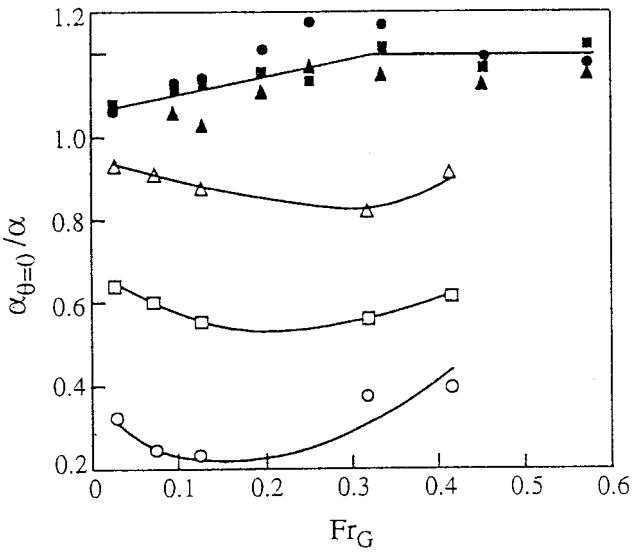

Fig. 7. Relative heat transfer coefficients at the top of horizontal and inclined tubes. Horizontal: ○ $Fr_L = 0.9$, □ $Fr_L = 1.3$, △ $Fr_L = 2.0$. Inclined at $\beta = 5°$: ● $Fr_L = 0.59$, ■ $Fr_L = 1.2$, ▲ $Fr_L = 2.0$.

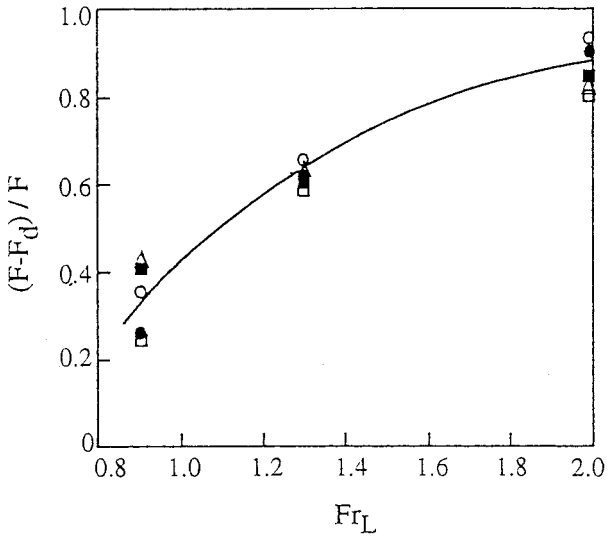

Fig. 8. Horizontal flow. Dependence of $F-F_d/F$ on Fr_L at the top of the tube: ○ $Fr_G = 0.03$, □ $Fr_G = 0.07$, △ $Fr_G = 0.13$, ● $Fr_G = 0.32$, ■ $Fr_G = 0.43$.

coefficient. It was obtained that dimensionless heat transfer coefficient α_θ/α_0 increases with increase of dimensionless angle θ from the top of the tube, so that the value of the wetted surface $((F-F_d)/F)$ also increases. The variation of $((F-F_d)/F)$ vs. θ is shown in Fig. 9a–c for liquid Froude number $Fr_L = 0.9$, 1.3, 2.0, respectively. The gas Froude number Fr_G varied from $Fr_G = 0.03$ to $Fr_G = 0.43$. The dryout was found to be dependent both on superficial liquid velocity and the angle θ. The lowest value of the wetted surface $((F-F_d)/F)$ was found at $Fr_L = 0.9$ at $\theta = 0$, whereas the highest $((F-F_d)/F)$ value was obtained at $Fr_L = 2.0$ at $\theta = 0.275$.

The circumferential variation of the dry surface may be described by a single line in the range of Froude number $Fr_L = 0.9$–2.0, using a non-dimensional parameter ψ

$$\psi = \frac{[(F_d)_0 - (F_d)_\theta]}{(F_d)_0} \tag{16}$$

where $(F_d)_0$ is the dry surface at $\theta = 0$, and (F_d) is the dry surface at θ. The results are shown in Fig. 10. The curve $\psi = f(\theta)$ describes all the runs with the standard deviation of 12% at $\theta = 0.0555$ and 0.110, and with the standard deviation of 5% in the range of $\theta = 0.165$–0.275.

Using results of dimensionless heat transfer coefficient and flow parameter fL/u_b the thermal bounding map was constructed at five different liquid Froude numbers $Fr_L = 0.59$, 0.90, 1.2, 1.3, 2.0 in the range of heat flux $q = 0.7$–53 kW/m^2. The gas Froude number varies in the range of $Fr_G = 0.03$–0.57. The results are shown in Fig. 11. The open signs represent points where dryout occurs (flow in horizontal tube) the closed signs represent points where dryout does not occur (flow in inclined tube at $\beta = 5°$). Periodicity of dryout produces a varying heat transfer coefficient at the top of the tube, and one would expect temperature fluctuations in

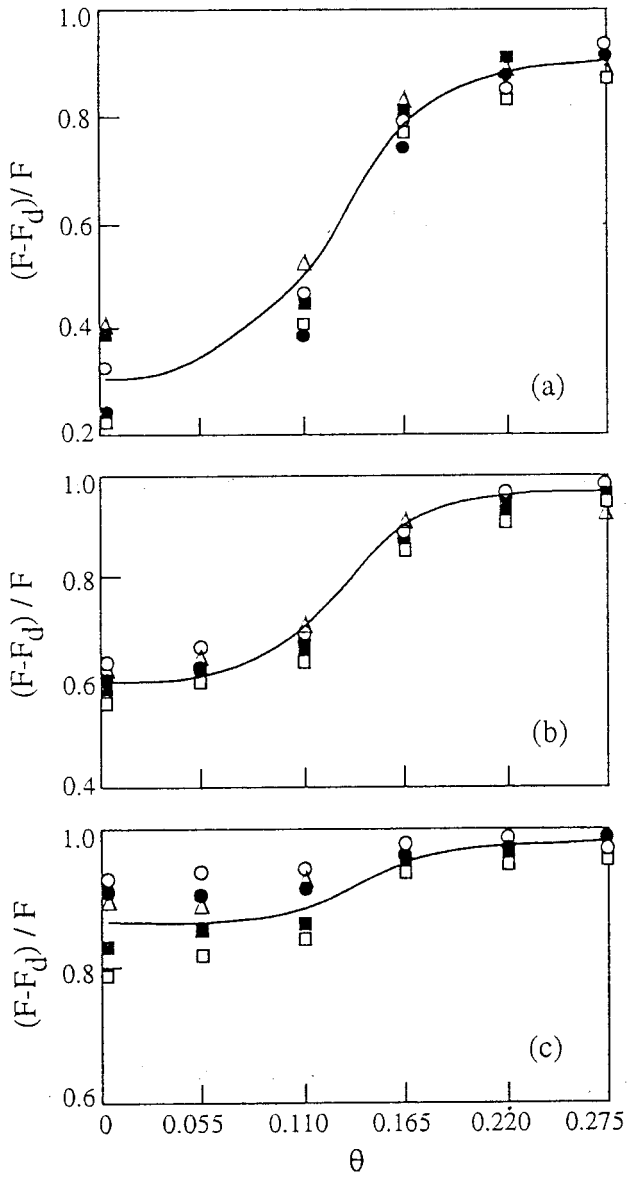

Fig. 9. Horizontal flow. Variation of $F-F_d/F$ vs. θ (a) $Fr_L = 0.9$, (b) $Fr_L = 1.3$, (c) $Fr_L = 2.0$ (○ $Fr_G = 0.03$, □ $Fr_G = 0.07$, △ $Fr_G = 0.13$, ● $Fr_G = 0.32$, ■ $Fr_G = 0.43$).

this case. The varying heat transfer coefficient was also observed in intermittent inclined flow; however, the presence of a transient dryout in horizontal flow leads to drastically increase in the amplitude of this fluctuation. Referring to Fig. 11, it is seen that for liquid Froude number $0.6 \leq Fr_L \leq 0.9$ the onset of intermittent flow dryout is inferred when flow parameter is in the range of $0.60 \leq fL/u_b \leq 0.75$.

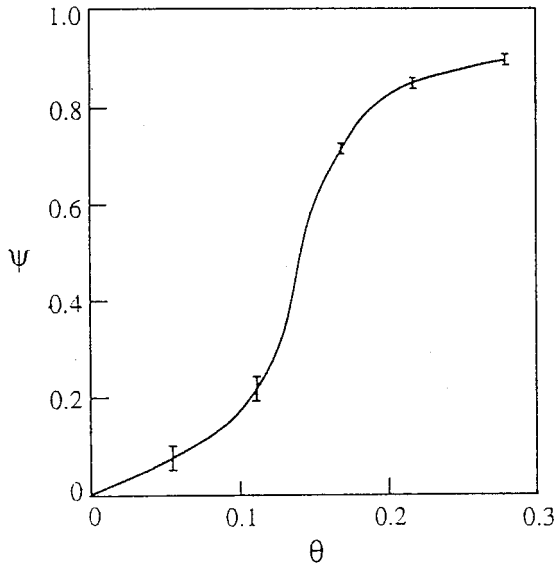

Fig. 10. Horizontal flow. Circumferential variation of dimensionless dry out surface $(F_d)_0 - (F_d)_0/(F_d)_0$.

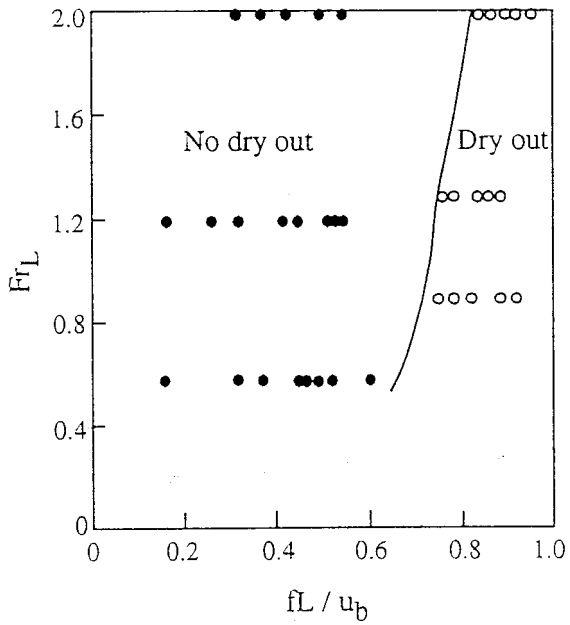

Fig. 11. Thermal bounding map: ● no dryout regime (flow in inclined tube), ○ dry out regime (flow in horizontal tube).

4.3. The temperature difference between the top and the bottom of a horizontal tube

The study of dryout has received great impetus because of its importance in the determination of maximum wall temperatures in a number of industrial applications. Thus, chemical process equipment, conventional power generation systems and refrigeration plants can all have dryout. The average (either spatial or temporal) heat transfer coefficient represents a macroscopic view of the process, and not a local instantaneous one. In applications, it is needed also to predict the wall temperature as a function of thermal-hydraulic conditions and time. It is often convenient to use dimensionless units for different pipes and different flow and thermal conditions. Since the experiments were carried out at the range of heat flux from 0.7 to 53 kW/m^2 we used a dimensionless temperature to similarity of the results. Their quantity is not depending on the value of heat flux and the fluid temperature.

The experimental results obtained are presented in the form of a graph showing the time variation of the dimensionless wall-temperature difference ϑ^+ between top and bottom of the pipe.

Two such examples, out of the many taken in the present study, are shown in Figs. 12 and

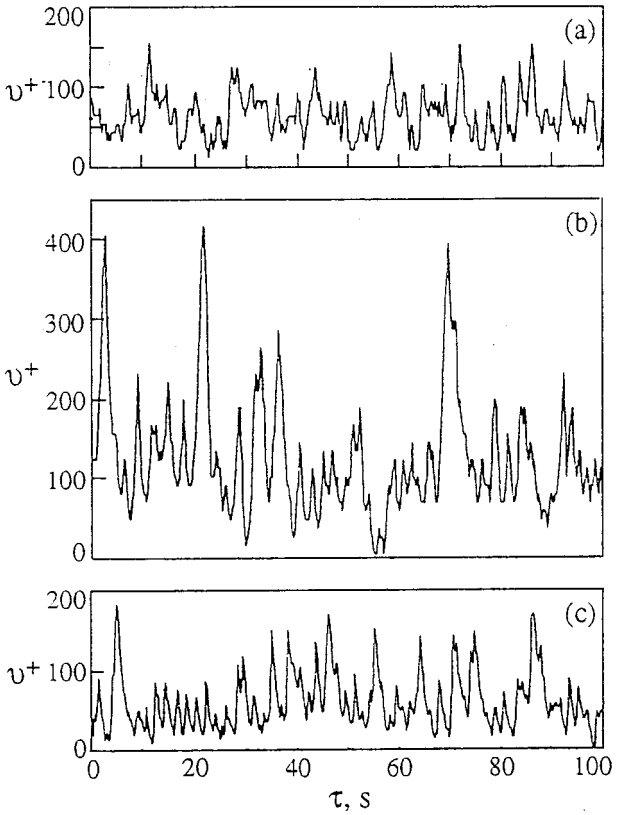

Fig. 12. Time variation of dimensionless temperature difference between top and bottom of the horizontal tube, $Fr_L = 0.9$: (a) $Fr_G = 0.03$, (b) $Fr_G = 0.13$ and (c) $Fr_G = 0.43$.

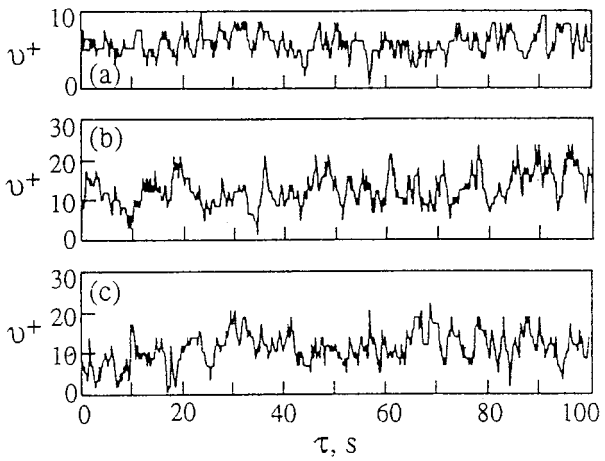

Fig. 13. Time variation of dimensionless temperature difference between top and bottom of the horizontal tube, $Fr_L = 2.0$: (a) $Fr_G = 0.03$, (b) $Fr_G = 0.13$ and (c) $Fr_G = 0.43$.

13 for liquid Froude numbers $Fr_L = 0.9$ ($U_{LS} = 0.62$ ms^{-1}) and $Fr_L = 2.0$ ($U_{LS} = 1.4$ ms^{-1}), respectively.

The following equations define the value of ϑ^+

$$\vartheta^+ = \frac{T_{\theta=0} - T_{\theta=2}}{\vartheta^*} \tag{17}$$

$$\vartheta^* = \frac{q}{\rho c_p u^*} \tag{18}$$

where $T_{\theta=0}$ and $T_{\theta=2}$ are the instantaneous wall temperature at the top of the tube, $\varphi = 0$, and the bottom, $\varphi = \pi$, respectively, ϑ^* is the reference temperature, q the heat flux, c_p,ρ, specific heat and density of water respectively, and u^* friction velocity. An advantage of this description is that the fluctuation of pipe temperature with time does not depend on heat flux. At $Fr_L = 0.90$ the time-average value of $\bar{\vartheta}^+$ increases from $\bar{\vartheta}^+ \approx 67$ to $\bar{\vartheta}^+ \approx 125$ when the gas Froude number increases from $Fr_G = 0.03$ to $Fr_G = 0.13$. In this case, the maximum of instantaneous value of ϑ^+_{max} increases from $\vartheta^+_{max} \approx 150$ (Fig. 12a) to $\vartheta^+_{max} \approx 400$ (Fig. 12b). When the gas Froude number continues to increase, the maximum of dimensionless temperature difference between top and bottom decreases and at $Fr_G = 0.43$ the values are $\vartheta^+_{max} \approx 170$ (Fig. 12c). At higher values of Fr_L the dimensionless temperature difference between top and bottom of the tube is not strongly affected by a change in gas Froude number. Fig. 13a–c show that at $Fr_L = 2.0$,$Fr_G = 0.03$–0.43, the time-average value of $\bar{\vartheta}^+$ changes from $\bar{\vartheta}^+ = 5$ to $\bar{\vartheta}^+ = 15$ and does not exceed the value of $\vartheta^+_{max} > 20$.

Fig. 14 shows the time-average value of $\bar{\vartheta}^+$ vs. Fr_G for all the experiments in horizontal air–water flow. The peak of ϑ^+ shifts to higher values of Fr_G with increase of the liquid Froude number. This peak is associated with minimum of relative heat transfer coefficient at the top of horizontal tube (Fig. 7).

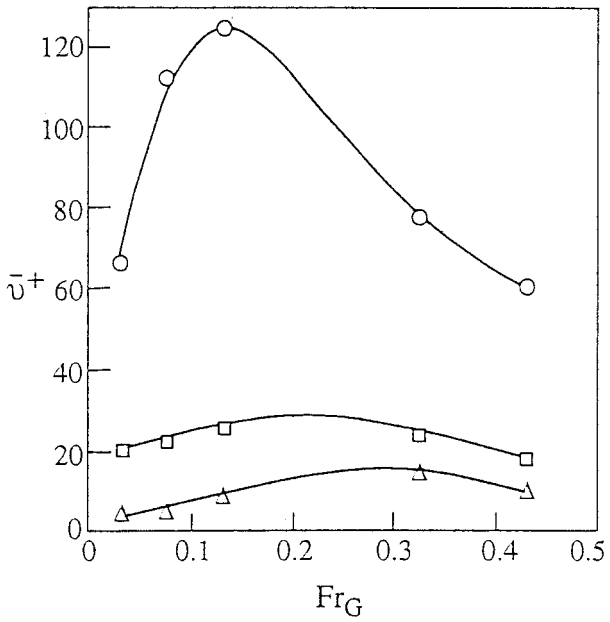

Fig. 14. Time-average dimensionless temperature difference between top and bottom of the horizontal tube ($\bar{\vartheta}^+$ vs. Fr_G): ○ $Fr_L = 0.9$ ($U_{LS} = 0.62$ m/s), □ $Fr_L = 1.3$ ($U_{LS} = 0.87$ m/s), △ $Fr_L = 2.0$ ($U_{LS} = 1.40$ m/s).

5. Discussion of the results

The definition of the dimensionless temperature is useful to predict temperature difference at the values of heat flux, which are different from those in the present experimental study. It is possible to calculate top to bottom temperature difference from Fig. 14 using heat flux as a parameter. Fig. 15 shows the time-average top to bottom temperature difference $\overline{\Delta T}$ vs. heat flux q. For superficial liquid velocity $U_{LS} = 0.62$ m/s ($Fr_L = 0.90$) in the range of superficial gas velocity $U_{GS} = 0.02$–0.30 m/s ($Fr_G = 0.03$–0.43) the $\overline{\Delta T}$ changes from 5–10 K at $q =$ 10 kW/m^2 to 40–90 K at $q = 100$ kW/m^2, depending on the gas Froude number. These values agree with experimental results presented by Bar-Cohen et al. (1987) and Crowe and Griffith (1993). The results obtained by Bar-Cohen et al. (1987) at superficial liquid velocity U_{LS} of about 0.6 m/s in the range of superficial steam velocity from 0.02 to 0.30 m/s showed that the maximum circumferential temperature difference is about 5–10 K at $q = 14$ kW/m^2. Crowe and Griffith (1993) showed that at $U_{LS} = 0.25$–0.35 m/s, and $U_{GS} = 0.2$–2 m/s $\overline{\Delta T}$ exceeded 50 K in the range of heat flux $q = 37$ to 71 kW/m^2. The maximum circumferential temperature difference decreases toward about 5 K at $q = 50$kW/m^2 when the U_{LS} increases up to 0.87 m/s (Fig. 15b) and nearly to vanish at the superficial liquid velocity of $U_{LS} = 1.4$ m/s ($Fr_L = 2.0$). We assume that the onset of dryout in intermittent flow is inferred when the $\overline{\Delta T}$ exceeds the value of $\overline{\Delta T} = 5$ K, at heat flux $q = 100$ kW/m^2. The value of heat flux $q = 100$ kW/m^2 is the highest in analysis of Bar-Cohen et al. (1987) to determine the values of superficial steam and liquid velocities at which the periodic, slug-driven liquid flow should be sufficient to prevent dryout of the upper surface of the pipe.

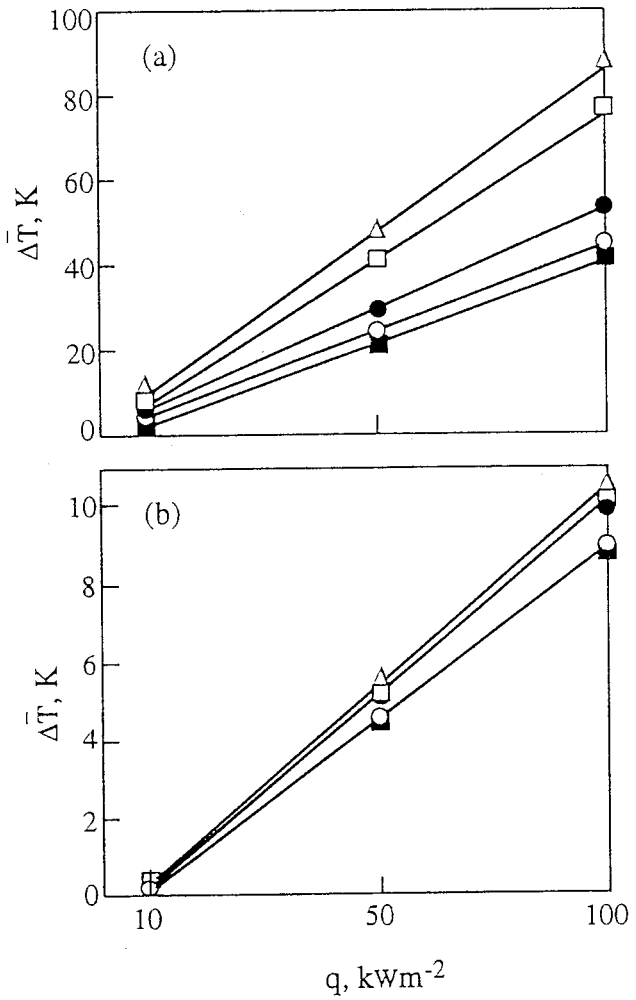

Fig. 15. Calculated values of time-average pipe anisothermality (top to bottom) at different values of heat flux (a) $Fr_L = 0.9$: ○ $Fr_G = 0.03$, □ $Fr_G = 0.07$, △ $Fr_G = 0.13$, ● $Fr_G = 0.32$; ■ $Fr_G = 0.43$ and (b) $Fr_L = 1.3$: ○ $Fr_G = 0.03$, □ $Fr_G = 0.07$, △ $Fr_G = 0.13$, ● $Fr_G = 0.32$; ■ $Fr_G = 0.43$.

In the present study, the conditions of $q = 100$ kW/m^2, $\overline{\Delta T} \leq 5$ K take place at superficial liquid velocity $U_{LS} = 1.4$ m/s ($Fr_L = 2.0$). Referring to Fig. 9, it is seen that in this case the relation of dryout surface to the whole heated surface is about 0.1 within the angle $\theta = 0$–0.11. It may be anticipated that at $Fr_L > 2$ dryout does not occur between slugs. This approach suggests that an analogy might exist between heat transfer in intermittent flow at $Fr_L > 2$, and full-pipe flow in a horizontal tube.

The extent of dryout would appear to depend on the balance between the forces working to rewet the same surface. To clarify this problem we studied heat transfer and flow parameters in horizontal and inclined tubes at the same liquid and gas Froude numbers. As previously shown such hydrodynamic parameters as holdup ε and the ratio of $R = fL/u_b$ are different for these

two cases. On the other hand, dryout does not occur in inclined tubes. We believe that from the experiments, it is possible to relate the existence of dryout to these flow parameters. These parameters are considered as acting separately, but are in fact dependent.

In Fig. 16 holdup in inclined air–water pipe flow is plotted relative to the values obtained for horizontal flow. Line of ratio $\varepsilon_{in}/\varepsilon_h = 1$ is shown for reference. The points are calculated from Figs. 3 and 4, which represent average values of holdup at different liquid Froude number with standard deviation of 20%. It can be seen that $\varepsilon_{in} > \varepsilon_h$, can be quite remarkable at $Fr_G > 0.07$. Thus, increase of holdup does not explain no dryout in inclined pipe at $Fr_G < 0.7$.

Fig. 17 contains the ratio of flow parameter $R_{in} = fL/u_b$ in inclined pipe to flow parameter $R_h = fL/u_b$ in horizontal pipe vs. gas Froude number. The points represent average values with standard deviation 15%. It is clear that the ratio R_{in}/R_h is less than unity in the whole range of liquid and gas Froude numbers of the present study.

6. Conclusion

We studied the dryout phenomena and heat transfer in air–water flow in horizontal and inclined tube at $\beta = 5^\circ$. The study was aimed at clarifying the relationship between hydrodynamic and dryout phenomena in intermittent air–water flow. It is shown that the high circumferential variation of the wall temperature that leads to dryout, takes place in a horizontal tube only. In the range of liquid Froude number $Fr_L = 0.9$–1.3 the horizontal tube was found to exhibit complex non-isothermal behavior. Alternatively, nearly isothermal pipe operation could be obtained by increasing the liquid Froude number to the high levels, $Fr_L = 2.0$. A method for calculating dryout in tube geometry has been presented. A two-phase

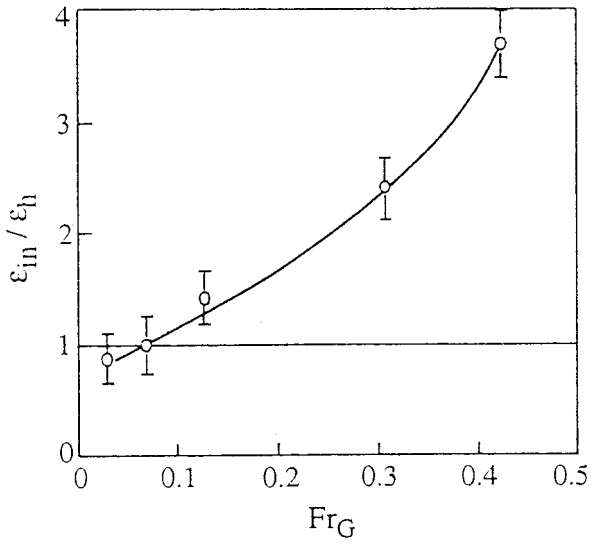

Fig. 16. The liquid holdup in inclined pipe divided by holdup in horizontal air–water pipe flow as a function of Fr_G.

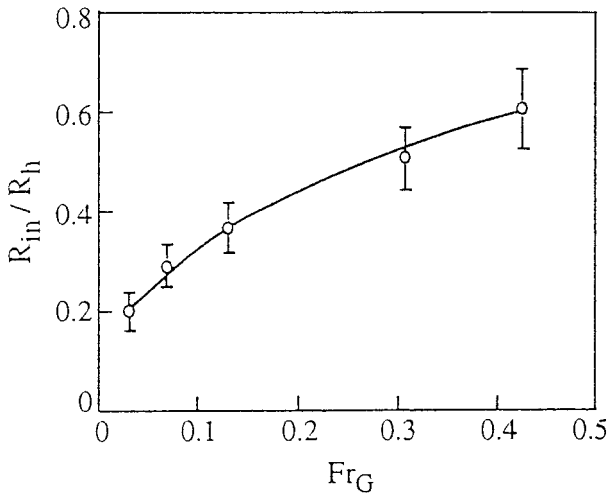

Fig. 17. The flow parameter $R_{in} = fL/u_b$ in inclined pipe divided by the flow parameter $R_h = fL/u_b$ in horizontal air–water pipe flow as a function of Fr_G.

model is utilized, which uses description of dryout based on the disappearance of the liquid film on the wall. The ratio of the time for gas phase to the total time for air and water mixture to pass the fixed point is a key phenomenon in dryout heat transfer. It was found that the parameter fL/u_b plays an important role in the prediction of dryout. For the horizontal tube, when dryout takes place, this parameter is of $fL/u_b > 0.7$. For the inclined tube, its value is less than 0.7 and dryout does not occur.

Acknowledgements

This research was supported by the Basic Research Foundation administered by the Israeli Academy of Sciences and Humanities, and by the Fund for the Promotion of Research at the Technion. This research is also supported by a grant from the German Federal Ministry of Education, Science, Research and Technology (BMBF) and the Israeli Ministry of Science (MOS) under the aegis of KFA-BEO-Forschungszentrum Jülich GmbH/Proektträger für Biologie, Energie, and Ökologie.

References

Andreussi, P., Asall, J.C., Hanratty, T.J., 1985. Initiation of roll waves in gas–liquid flow. AIChE J 31, 119–126.

Andreussi, P., Minervi, A., Paglanti, A., 1993. Mechanistic model of slug flow in near horizontal pipelines. Int. J. Multiphase Flow 39, 1281–1291.

Andritsos, N., Hanratty, T.J., 1987. Interfacial instabilities for horizontal gas–liquid flows in pipelines. Int. J. Multiphase Flow 13, 565–575.

Bar-Cohen, A., Ruder, Z., Griffith, P., 1987. Thermal and hydrodynamic phenomena in a horizontal, uniformly heated steam-generating pipe. J. Heat Transfer 109, 739–745.

Barnea, D., Taitel, Y., 1986. Flow pattern transition in two-phase gas–liquid flows. In: Cheremisinoff, N.P. (Ed.), Encyclopedia of Fluid Mechanics, Part 3. Gulf publishing, Houston.

Barnea, D., Taitel, U., 1993. A model for slug length distribution in gas–liquid slug flow. Int. J. Multiphase Flow 19, 829–838.

Chan, A.M.C., Banerjee, S., 1981. Refilling and rewetting of a hot horizontal tube. Part 3: Application of a two-fluid model to analyze rewetting. Trans. ASME J. Heat Transfer 103, 653–659.

Coney, M.W.E., 1974. The analysis of a mechanism of liquid replenishment and draining in horizontal two-phase flow. Int. J. Multiphase Flow 1, 647–669.

Crowe, K.E., Griffith, 1993. Intermittent flow dryout limit in heated horizontal tubes. Int. J. Multiphase Flow 19, 575–588.

Delhaye, J.M., 1981. Basic equations for two-phase flow modeling (Chapt. 2). In: Two-phase Flow and Heat Transfer in the Power and Process Industries. Hemisphere and McGraw-Hill, New York, pp. 40–97.

Dukler, A.E., Hubbard, E.G., 1975. A model for gas–liquid slug flow in horizontal and near-horizontal tubes. Ind. Eng. Chem. Fundam 14, 337–347.

Elias, E., Yadigaroglu, G., 1977. A general one-dimensional model for conduction controlled rewetting of a surface. Nucl. Eng. Design 42, 185–194.

Fisher, S.A., Yu, S.K.M., 1975. Dryout in serpentine evaporates. Int. J. Multiphase Flow 1, 771–791.

Grolman, E., Fortuin, J.M.H., 1997a. Liquid hold-up, pressure gradient and flow patterns in inclined gas–liquid pipe flow. Experimental Thermal and Fluid Science 15, 174–182.

Grolman, E., Fortuin, J.M.H., 1997b. Gas–liquid flow in slightly inclined pipes. Chem. Eng. Sci 52, 4461–4471.

Hahne, E., Herrmann, U., Rheinlander, J., 1997. The effect of tilt on flow patterns of water/steam flow through heated tubes. In: Giot, M., Mayinger, F., Celata, G.P. (Eds.), Experimental Transfer, Fluid Mechanics and Thermodynamics. Edizioni PISA ETS, pp. 925–934.

Hand, N.P., Spedding, P.L., Ralph, S.J., 1992. The effect of surface tension on flow pattern, holdup and pressure drop during horizontal air–water pipe flow at atmospheric conditions. Chem. Eng. J 48, 197–210.

Hand, N.P., Spedding, P.L., 1993. Horizontal gas–liquid flow at close to atmospheric conditions. Chem. Eng. Sci 48, 2283–2305.

Hanratty, T.J., Hershmann, A., 1961. Initiation of roll waves. AIChE J 7, 488–497.

Hetsroni, G., 1982. Handbook of Multiphase Systems. Hemisphere, Washington, DC.

Hetsroni, G., Rozenblit, R., 1994. Heat transfer to a liquid–solid mixture in a flume. Int. J. Multiphase Flow 20, 671–689.

Hetsroni, G., Rozenblit, R., Yarin, L.P., 1996. A hot-foil infrared technique for studying the temperature field on a wall. Measurements Sci. and Technol 7, 1418–1427.

Hetsroni, G., Hu, B.G., Yi, J.H., Mosyak, A., Yarin, L.P., Ziskind, G., 1998a. Heat transfer in intermittent air–water flows. Part 1: Horizontal tube. Int. J. Multiphase Flow 24, 165–188.

Hetsroni, G., Hu, B.G., Yi, J.H., Mosyak, A., Yarin, L.P., Ziskind, G., 1998b. Heat transfer in intermittent air–water flows. Part 2: Upward inclined tube. Int. J. Multiphase Flow 24, 189–212.

Hewitt, G.F., Wallis, G.B., 1974. Flooding and associated phenomena in falling flow in a vertical tube. In: ASME Winter Annual Meeting, Multiphase Flow Symposium, Philadelphia, PA.

Ishii, M., 1975. Thermo-Fluid Dynamic Theory of Two-Phase Flow. Eyrolles, Paris.

Jepson, W.P., Taylor, R.E., 1993. Slug flow and its transition in large-diameter horizontal pipes. Int. J. Multiphase Flow 19, 411–420.

Kokal, S.L., Stanislav, 1989. An experimental study of two-phase flow in slightly inclined pipes. Part II: Liquid holdup and pressure drop. Chem. Eng. Sci 44, 681–693.

Lin, P.Y., Hanratty, T.J., 1987a. Detection of slug flow from pressure measurements. Int. J. Multiphase Flow 13, 13–21.

Lin, P.Y., Hanratty, T.J., 1987b. Effect of pipe diameter of flow pattern for air-water flow in horizontal pipes. Int. J. Multiphase Flow 13, 537–553.

Nadler, M., Mewes, D., 1995. Effects of the liquid viscosity on the phase distributions in horizontal gas–liquid slug flow. Int. J. Multiphase Flow 21, 253–266.

Nelson, R.A., Pasamehmetoglu, K.O., 1992. Quenching phenomena. In: Hewitt, G.F., Delhaye, J.M., Zuber, N. (Eds.), Post-Dryout Heat Transfer. CRC Press, Boca Raton, FL, pp. 39–184.

Nicholson, M.K., Aziz, K., Gregory, G.A., 1978. Intermittent two-phase flow in horizontal pipes: predictive models. Can. J. Chem. Eng 56, 653–663.

Ruder, Z., Bar-Cohen, A., Griffith, P., 1986. An example of the application of the bounding dryout criteria in horizontal steam generating tubes for the case of circumferentially nonuniform heat flux. Int. J. Multiphase Flow 12, 845–852.

Ruder, Z., Hanratty, P.J., Hanratty, T.J., 1989. Necessary conditions for the existence of stable slugs. Int. J. Multiphase Flow 15, 209–226.

Singh, G., Griffith, P., 1970. Determination of the pressure drop optimum pipe size for a two-phase slug flow in an inclined pipe. J. Eng. Trans. ASME 92, 717–726.

Taitel, Y., Dukler, A.E., 1976. A model for predicting flow regime transitions in horizontal and near horizontal gas–liquid flows. AIChE J 22, 47–55.

Taitel, Y., Barnea, D., 1990. A consistent approach for calculating pressure drop in inclined slug flow. Chem. Eng. Sci 45, 1199–1206.